

Damage Limit of Concrete Filled Steel Tube Frame under Strong Ground Motion



15 WCEE
LISBOA 2012

K. Goto

Miyakonojo National College of Technology, Japan

SUMMARY:

In this study seismic response and damage limit of CFT frame are investigated in relation with the ultimate state design conditions which are the column-over-design factor of frame, the strength ratio of CFT column and the maximum velocity of input ground motion. The numerical analysis method to predict the damage of CFT frame is obtained by introducing the damage ratios of the steel tube cracking and local buckling of CFT column and the cracking fracture of H-section beam. By the use of the presented analysis method, the seismic responses of CFT frame designed under quite different design conditions are calculated and the damage ratios of CFT frame are obtained quantitatively for each design condition in this paper.

Keywords: Concrete filled steel tube, Cracking, Local buckling, Multi story frame, Column over design factor

1. INTRODUCTION

It is well known that the concrete filled steel tube column (CFT column) is ductile and useful member as earthquake resistant element. In some case, however, CFT column fractures because of the cracking of steel tube while under strong seismic load. This fracture is brittle and predicted to be worked to collapse of CFT frame. From this reason, seismic response collapse and cracking damage of CFT frame, which is composed of CFT columns and H-section beams, have been investigated. Seismic response collapse of multi-story CFT frame is closely related to the fracture of structural members, especially to fracture of columns (Saisho & Goto 2004, Goto & Saisho 2010). Therefore, the restoring force characteristics and fracture mechanism of CFT column caused from steel tube cracking have been studied, and restoring force model and cracking condition of it were obtained (Saisho & Goto 2001). In this study, using the cracking analysis methods, seismic response and strength ratio limit of CFT frame are investigated in relation with the ultimate state design conditions which are the column-over-design factor of frame (r_{cb}), the distribution of r_{cb} and the maximum velocity of input ground motion to prevent the local buckling and cracking of CFT column subjected to strong seismic load.

2. SEISMIC RESPONSE ANALYSIS METHOD OF CFT FRAME

2.1 CFT frame model

In the dynamic collapse analysis of CFT frame, the multi-story plane frame is assumed to be composed of the rigid panel zones of beam-to-column connection and the axially elastic members with elastic-plastic hinges at both ends as explained in Fig. 2.1 (Saisho & Goto 2004). The mass of frame is concentrated in every panel zone and distributed uniformly in it. The displacement of frame can be expressed only by the rotation (θ_i , i : number of panel zone), the horizontal displacement (u_i) and the vertical displacement (w_i) of every rigid panel zone. The viscous damping of frame is expressed by the Rayleigh Damping in which the damping factors of the first mode (h_1) and the second mode (h_2) are assumed to be $h_1 = 0.02$ and $h_2 = 0.02$.

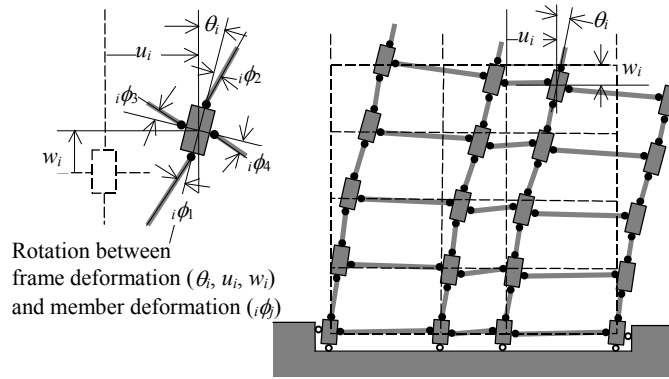


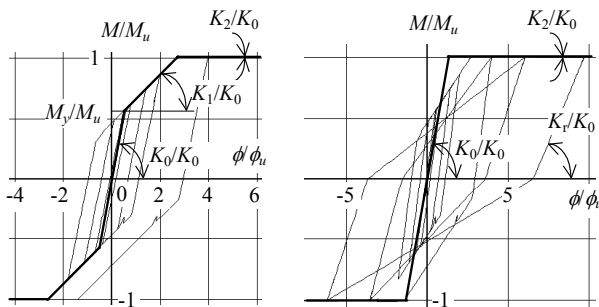
Figure 2.1. CFT frame model for numerical analysis

2.2 Restoring force characteristic and model of CFT column

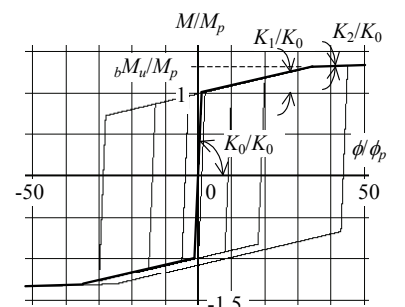
The restoring force model of elastic-plastic hinge is obtained on the basis of the dynamic loading tests of CFT column (Saisho & Goto 2001). According to the test results the non-dimensional restoring force (M/M_u) of CFT column until the local buckling of steel tube is approximated by the Tri-linear model whose skeleton curve is explained in Fig 2.2 (a). After the local buckling of steel tube, it is expressed by the Clough model (Clough & Johnston 1966) as shown in Fig 2.2 (b). The stiffness ratios at the plastic range in Fig. 2.2 are given as $K_1/K_0 = 0.2$, $K_2/K_0 = 0.001$ which are approximated on the basis of the test results. The restoring force models mentioned above are defined by the non-dimensional restoring force (M/M_u) in which the ultimate bending strength (M_u) changes at every moment by the varying axial force of CFT column. Accordingly the restoring force model can simulate the effect of varying axial force of CFT column.

2.3 Restoring force characteristic and model of H-section beam

The H-section beam of multi-story CFT frame is also expressed by the axially elastic member with the elastic-plastic hinges at both ends as shown in Fig. 2.1. The restoring force of the elastic-plastic hinge is decided by the Tri-linear model shown in Fig. 2.3 in which the restoring force characteristics are given by the full plastic moment (M_p) and the ultimate bending strength (${}_bM_u$) of H-section beam. The strain hardening behavior of H-section beam affects the seismic response and collapse of CFT frame under strong ground motion. Accordingly the strain hardening of H-section beam in the model can not be neglected. It is given by the K_1 -value which is obtained by assuming H-section beam is approximated by two-flange section member.



(a) Before local buckling ($K_1/K_0=0.2, K_2/K_0=0.001$)
 (b) After local buckling ($K_2/K_0=0.001, K_r/K_0$: unloading stiff.)



(K_1/K_0 : Eqn. (2.1), $K_2/K_0=0.001, \phi_p=M_p/K_0$)

Figure 2.2 Restoring force models of CFT column

Figure 2.3 Restoring force model of H-section beam

$$\frac{K_1}{K_0} = \frac{1/y - 1}{1.5y(1-y)(1+u) - 1} \quad (2.1)$$

where y ($= \sigma_y/\sigma_u$) and u ($= \varepsilon_u/\varepsilon_y$) mean the yield stress ratio and the ultimate tensile strain ratio respectively.

2.4 Strong ground motion

To calculate the seismic response and damage of CFT frame, El-Centro (California 1940), Taft (California 1952), Hachinohe (Aomori, Japan 1968) and JMA-Kobe (Kobe, Japan 1997) are used as input ground motion. These time histories of acceleration and acceleration response spectra are shown in Figs. 2.4 – 2.5 respectively.

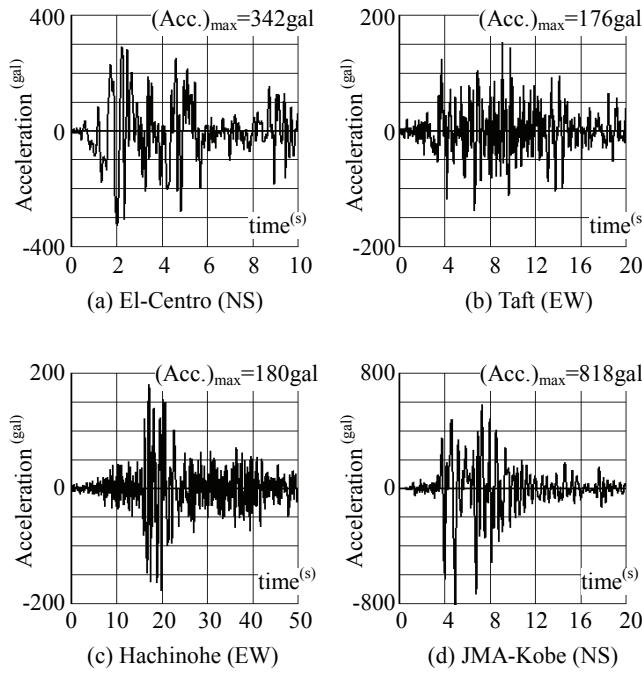


Figure 2.4 Time histories of input ground motions

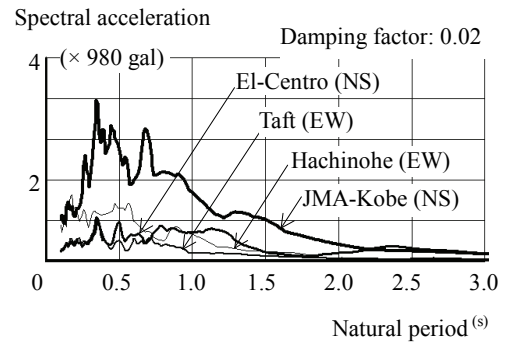


Figure 2.5 Response spectra of input ground motions

3. DESIGN OF CFT FRAME

3.1 Design conditions of CFT frame with uniform column-over-design factor

CFT frames to be calculated in this study are the 15-story 3-bay frames and 7-story 3-bay frames. They are designed under the following conditions.

- i) The distribution of story shear strength ratio is decided by the Japanese design code. The base shear strength coefficient C_B ($= Q_1/W$, Q_1 : ultimate shear force of the first story, W : weight of frame) of 15-story frame and 7-story frame are also decided by the design code and they are $C_B = 0.25$ and $C_B = 0.40$ respectively. The frame strength is calculated by the limit analysis assuming the collapse mechanism of frame with plastic hinges at every beam-end and the upper and lower column-ends in the top story and the first story.
- ii) The column-over-design factor (r_{cb}) of every beam-to-column connection except for the highest story is the same and they are $r_{cb} = 1.0 - 6.0$.

iii) The strength ratio of filled concrete to steel tube $\rho (= \sigma_c A_c / \sigma_u A_s, A_c, A_s : \text{sectional areas of concrete and steel tube respectively, } \sigma_c : \text{compression strength of filled concrete, } \sigma_u : \text{tensile strength of steel tube})$ affects the restoring force characteristics of CFT column strongly (Saisho & Goto 2001). From this reason the strength ratios (ρ) of all CFT columns are assumed to be the same in the frame and they are $\rho = 0.5 - 16.0$ in this study.

iv) Every H-section beam of multi-story frame satisfies the critical conditions of the width-to-thickness ratio of flange (b/t_f) and web (h/t_w) and the lateral buckling parameter ($L_b h/A_f$). They are $b/t_f = 5, h/t_w = 71$ and $L_b h/A_f = 375$ ($b : \text{half width of flange, } h : \text{depth of beam, } t_f, t_w : \text{thicknesses of flange and web respectively, } A_f : \text{sectional area of flange, } L_b : \text{beam length}$).

All CFT frames are designed under the conditions mentioned above and another condition that any dimensions of steel tube and H-section are available. The story-height of every CFT frame is 4.0 m and the span lengths of outer span and inner span are 8.0 m and 6.0 m respectively. The weight of each story is 2000 kN. The yield stress (σ_y) and the tensile strength (σ_u) of steel tube and H-section beam are $\sigma_y = 340 \text{ N/mm}^2$ and $\sigma_u = 440 \text{ N/mm}^2$. The fracture elongation (ε_f) of steel tube and H-section beam is $\varepsilon_f = 0.20$. The compression strength of filled concrete (σ_c) is $\sigma_c = 30, 60, 120 \text{ N/mm}^2$.

Some results of designed CFT frames are shown in Figs. 3.1 – 3.2 in which there are diameter (D) of CFT column, depth (H) of H-section beam at the first story and natural period (T) of CFT frame. All D and H are practical dimensions and T are mostly constant. From these results it is ascertained that the design method of multi-story CFT frame in this study is useful.

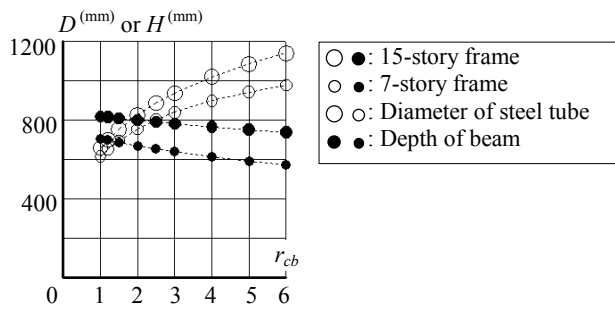


Figure 3.1 Members' dimensions of CFT frames with uniform r_{cb}

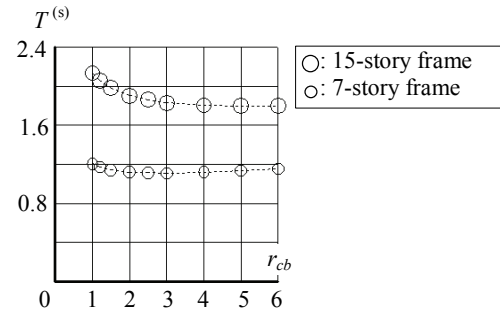


Figure 3.2 Natural periods of CFT frames with uniform r_{cb}

3.2 Design condition of CFT frame with uneven column-over-design factor

It is well known that r_{cb} is an important earthquake resistant design factor of multi-story frame. Saisho and Goto (2004) pointed out the necessary value of r_{cb} to prevent the local buckling of CFT column and that value is $r_{cb} = 2$. This necessary value was obtained by the seismic response analyses of many CFT frames designed as r_{cb} is distributed uniformly at every beam-to-column connection. However, r_{cb} is distributed unevenly in real multi-story frame. Accordingly, to study the relation between distribution of r_{cb} and distribution of damage, many CFT frames are designed and analyzed in this paper. The design condition of CFT frame are the same with before section except for design condition ii). Only design condition ii) concerning r_{cb} is changed as below.

ii-1) The column-over-design factor (r_{cb}) of every beam-to-column connection except for the highest story is designed as shown in Fig. 3.3.

in which,

A-frame : r_{cb} are varied at some upper stories.

B-frame : r_{cb} are increased from the lowest story monotonically and linearly.

C-frame : r_{cb} are decreased from the lowest story monotonically and linearly.

Some design results are shown in Table 3.1 in which there are diameter (D) of CFT column, depth (H) of H-section beam at the first story, natural period (T) and all members' weight ratio (r_w) of uneven frame to uniform frame whose r_{cb} is 3.

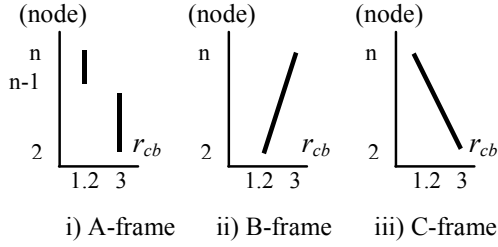


Figure 3.3 Distribution of r_{cb}

Table 3.1 Designed CFT frames with uneven r_{cb}

Frames	D	H	T	r_w
15-uniform ($r_{cb} = 3$)	937	782	1.83	1.000
15-A	912	755	1.88	0.962
15-B	798	968	2.07	0.769
15-C	846	680	1.92	0.853
7-uniform ($r_{cb} = 3$)	840	640	1.11	1.000
7-A	781	580	1.13	0.900
7-B	729	811	1.24	0.794
7-C	765	564	1.10	0.871

D : Diameter of steel tube (mm), H : Depth of beam (mm)
 T : Natural period (s), r_w : ratio of members' weight

4. DAMAGE RATIO EQUATION OF CFT COLUMN AND H-SECTION BEAM

4.1 Damage ratio equation of CFT column

From the cyclic loading tests of CFT column it is shown that the steel tube of CFT column cracks and fractures as shown in Fig. 4.1 (a) when the accumulated plastic strain of steel tube becomes to be equal to the critical value ($\alpha\varepsilon_f$). From this result the cracking condition is expressed by Eqn. 4.1 (Saisho & Goto 2001).

$$\sum \varepsilon_{TC} + \sum \varepsilon_T = \alpha\varepsilon_f \quad (4.1)$$

where ε_T : the plastic tension strain of steel tube in the tension stress side, ε_{TC} : the plastic tension strain due to the local buckling deformation of steel tube in the compression stress side, $\alpha (= -0.3\rho + 5.0)$: constant expressed by the strength ratio of filled concrete to steel tube (ρ), ε_f : fracture elongation of steel tube, Σ : summation of plastic strain under cyclic load. From Eqn. 4.1, the cracking damage ratio of CFT column (${}_cD_{cr}$) is expressed by Eqn. 4.2.

$${}_cD_{cr} = (\sum \varepsilon_{TC} + \sum \varepsilon_T) / \alpha\varepsilon_f \quad (4.2)$$

As shown in Eqn. 4.1, the local buckling of steel tube (Fig. 4.1 (b)) is closely related to the steel tube cracking. The local buckling condition is obtained on the basis of the upper bound theorem of the limit analysis (Saisho et al. 2004). The damage ratio of local buckling (${}_cD_{lb}$) is decided by the use of critical deformation (${}_c\delta_{lb}$) that corresponds to the CFT column deformation for the steel tube to buckle locally.

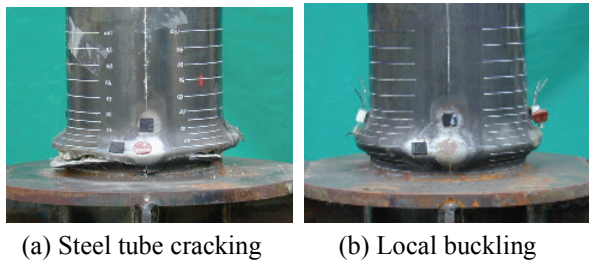


Figure 4.1 Steel tube cracking and local buckling of CFT column

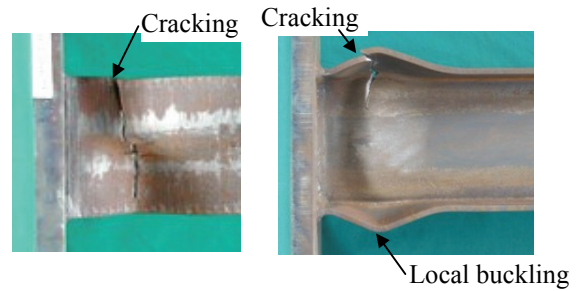


Figure 4.2 Cracking and local buckling of H-section beam

$${}_c D_{lb} = |{}_c \delta_{pc} - {}_c \delta_{pt}| / {}_c \delta_{lb} \quad (4.3)$$

where ${}_c \delta_{pc} - {}_c \delta_{pt}$ is the amplitude of plastic deformation of CFT column.

4.2 Damage ratio equation of H-section beam

When strong alternating repeated load is applied to the H-section cantilever beam, flange buckles locally and after that cracks (Fig. 4.2) even if the fracture at the welded joint is avoided. According to the dynamic loading tests of H-section cantilever beam, the cracking fracture of H-section beam is considered as the very low-cycle fatigue behavior and assumed to be approximated by the Palmgren-Miner rule (Goto 2010, Goto & Saisho 2010). From the Palmgren-Miner rule, the damage ratio is given by the accumulation of each cycle damage (Dowling 2007). Therefore, the cracking damage ratio of H-section beam (${}_b D_{cr}$) in each instant under random repeated load can be expressed by Eqn. 4.4.

$${}_b D_{cr} = \sum_j \frac{1}{N_{jf}} \quad (4.4)$$

where N_{jf} means the number of cycle to fracture under j -th cycle load and N_f is approximated by the Coffin-Manson relationship as shown in Eqn. 4.5.

$$\varepsilon_{pa} = \varepsilon_f (2N_f)^c \quad (4.5)$$

where ε_{pa} : the plastic strain amplitude of H-section beam flange (Goto & Saisho 2010), ε_f : fracture elongation, c : material modulus.

The local buckling condition of flange at the beam end is obtained on the basis of the upper bound theorem of the limit analysis (Goto 2010). The damage ratio of local buckling (${}_b D_{lb}$) is decided by the use of critical deformation (${}_b \delta_{lb}$).

$${}_b D_{lb} = |{}_b \delta_{pc} - {}_b \delta_{pt}| / {}_b \delta_{lb} \quad (4.6)$$

where ${}_b \delta_{pc} - {}_b \delta_{pt}$ is the amplitude of plastic deformation of H-section beam.

5. SEISMIC RESPONSE ANALYSIS AND EFFECT OF COLUMN-OVER-DESIGN FACTOR

5.1 Effect of column-over-design factor on maximum damage ratios of CFT frame

The damage distributions of CFT frames ($\rho = 3$, $\sigma_c = 60 \text{ N/mm}^2$) under JMA-Kobe are shown in Fig. 5.1. The column-over-design factors (r_{cb}) of these CFT frames are distributed uniformly. The damages of CFT frame are the story deformation angle (Δ/L), the local buckling damage ratios of CFT column (${}_c D_{lb}$) and H-section beam (${}_b D_{lb}$) and the cracking damage ratios of CFT column (${}_c D_{cr}$) and H-section beam (${}_b D_{cr}$). To show the effect of r_{cb} , calculations in these figures are carried out under the condition of $r_{cb} = 1.2, 2, 3, 6$.

Although all CFT frames are designed under the same design conditions on the ultimate story shear strength, the strength distribution along the story and the strength ratio of filled concrete to steel tube (ρ), we can see the remarkable differences of the damage ratio distribution among the CFT frames. In the CFT frames of $r_{cb} = 1.2$, many CFT columns buckle locally ($({}_c D_{lb})_m = 1.0$) and high cracking damage ratios of CFT column appear. On the other hand, the local buckling of CFT column does not appear in the CFT frame of $r_{cb} = 6$. Therefore, the cracking damage ratios of CFT columns are low.

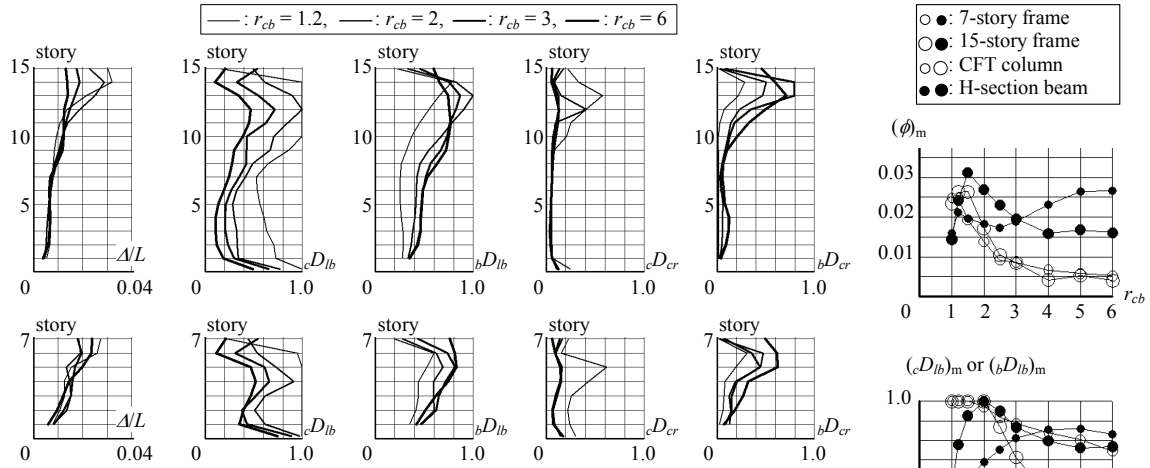


Figure 5.1 Damage distributions of CFT frame, whose r_{cb} -values are distributed uniformly, under JMA-Kobe

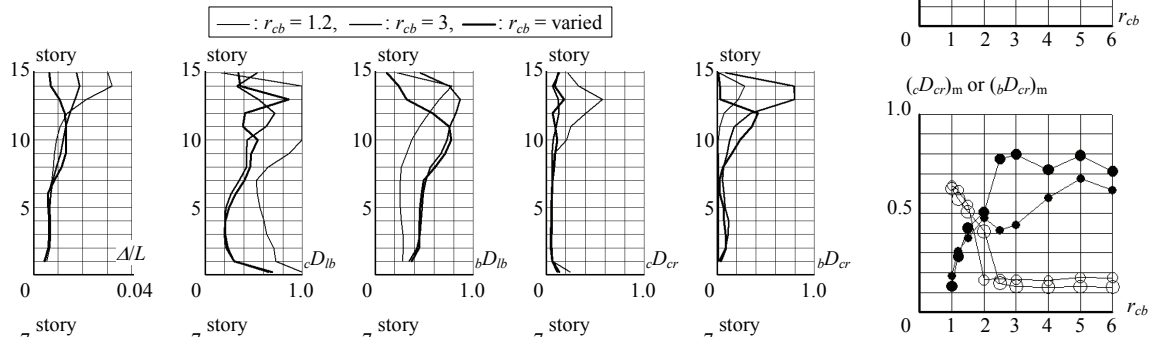


Figure 5.2 Effect of r_{cb} on the maximum damages of CFT frame ($\rho = 3$, $\sigma_c = 60 \text{ N/mm}^2$) under JMA-Kobe

Figure 5.3 Damage distributions of A-frame under JMA-Kobe

The relations between r_{cb} and the maximum rotation of elastic-plastic hinge of members $(\phi)_m$ and the maximum damage ratios $((cD_{lb})_m, (bD_{lb})_m, (cD_{cr})_m, (bD_{cr})_m)$ of CFT frame ($\rho = 3$, $\sigma_c = 60 \text{ N/mm}^2$) under JMA-Kobe are explained in Fig. 5.2. According to Fig. 5.2, the complicated differences due to the design conditions are observed but the maximum damage ratios of $(cD_{lb})_m$ and $(cD_{cr})_m$ increase monotonically in most cases with decreasing of r_{cb} . Especially, it is observed $(cD_{cr})_m$ increase remarkably when the local buckling of CFT column occurs ($(cD_{lb})_m = 1.0$). On the other hand, $(bD_{cr})_m$ tends to increase with r_{cb} , however, H-section beam does not crack even if $r_{cb} = 6$. From these results, it is shown that the maximum damage ratios of CFT column are clearly affected by r_{cb} .

5.2 Effect of distribution of column-over-design factor

5.2.1 A-frame

From the calculated results shown in Fig.5.1, the damage ratios of H-section beams at the upper stories become high even if the column-over-design factor (r_{cb}) is high. Accordingly r_{cb} are varied at the upper nodes where 15-story frame is the 14th and 15th nodes and 7-story frame is 6th and 7th nodes (see Fig. 3.3) to degrade damages of H-section beams at the upper stories. Fig. 5.3 shows the maximum damage distributions of CFT frames ($\rho = 3$, $\sigma_c = 60 \text{ N/mm}^2$) under JMA-Kobe. From these calculated results, $(bD_{cr})_m$ are improved at the upper stories. However, the damage ratios of CFT columns near the upper stories increase. Accordingly it is pointed out that the sudden change of r_{cb} provides not good design condition.

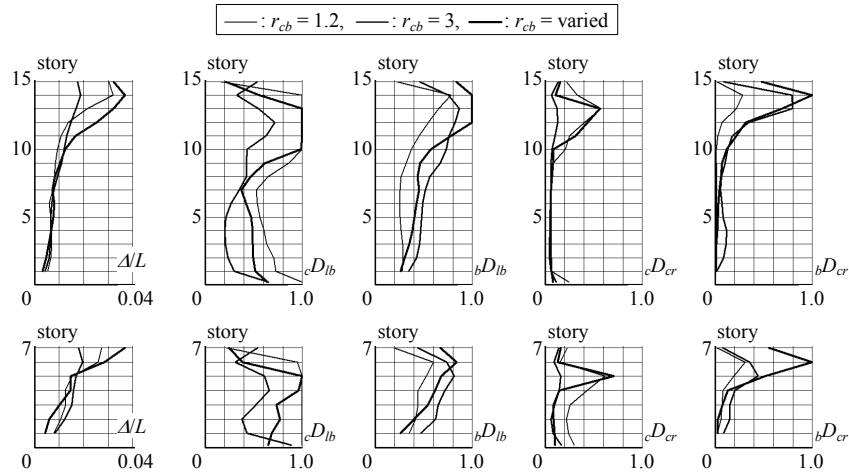


Figure 5.4 Damage distributions of B-frame under JMA-Kobe

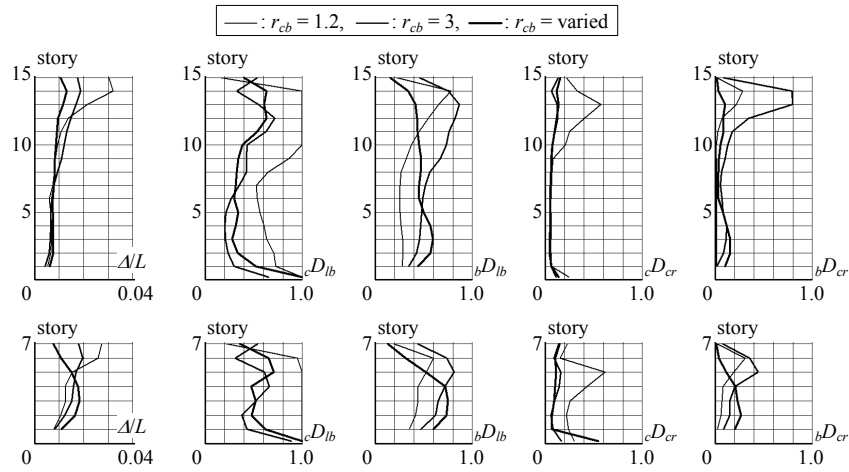


Figure 5.5 Damage distributions of C-frame under JMA-Kobe

5.2.2. B-frame

To avoid damage concentration at specific stories, r_{cb} are increased from the first story ($r_{cb} = 1.2$) to the highest story ($r_{cb} = 3.0$) monotonically and linearly (see Fig. 3.3). Fig. 5.4 shows the maximum damage distributions of CFT frames ($\rho = 3$, $\sigma_c = 60 \text{ N/mm}^2$) under JMA-Kobe. From the calculated results, the local buckling and cracking damage ratios of members are high because the maximum deformation angle (Δ/L) are higher than the CFT frame of $r_{cb} = 1.2$. These results show that there is a not safe design distribution of r_{cb} even if the frame is designed with enough high r_{cb} at some stories.

5.2.3. C-frame

CFT frames whose r_{cb} are decreased from the first story ($r_{cb} = 3.0$) to the highest story ($r_{cb} = 1.2$) monotonically and linearly (see Fig. 3.3) have been analyzed. Fig. 5.5 shows the maximum damage distributions of CFT frames ($\rho = 3$, $\sigma_c = 60 \text{ N/mm}^2$) under JMA-Kobe. Although high local buckling damage ratio of CFT column at the first story appears, other damage ratios of CFT columns and H-section beams are low enough and distributed uniformly. These results show that there is a safe design distribution of r_{cb} .

6. SEISMIC RESPONSE ANALYSIS AND EFFECT OF STRENGTH RATIO OF CFT COLUMN

To show the effect of the strength ratio of filled concrete to steel tube (ρ) on the maximum damage

ratios of CFT frame ($(\phi)_m$, $(cD_{lb})_m$, $(bD_{lb})_m$, $(cD_{cr})_m$, $(bD_{cr})_m$), seismic response analyses of CFT frames with variable ρ are carried. Fig.6.1 shows the some calculated results as examples. According to Fig. 6.1, the complicated differences are observed. But $(cD_{lb})_m$ and $(cD_{cr})_m$ increase monotonically with ρ . It is also observed that the upper bounds of ρ not to occur the local buckling and the steel tube cracking of CFT column exists and these bounds are strongly affected by the column-over-design factor (r_{cb}).

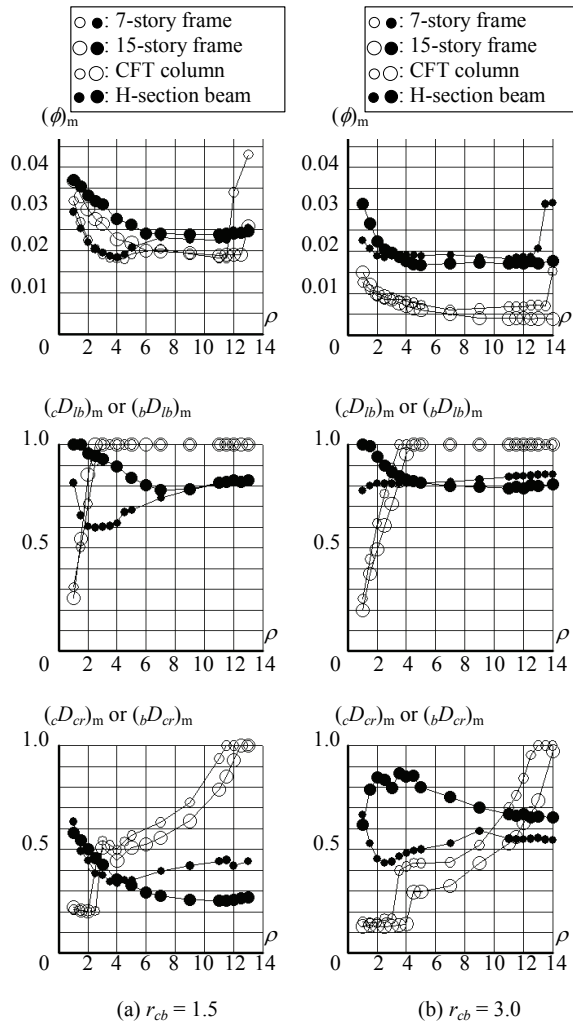


Figure 6.1 Effect of the strength ratio of filled concrete to steel tube (ρ) on the maximum damages of CFT frame ($\sigma_c = 60 \text{ N/mm}^2$) under JMA-Kobe

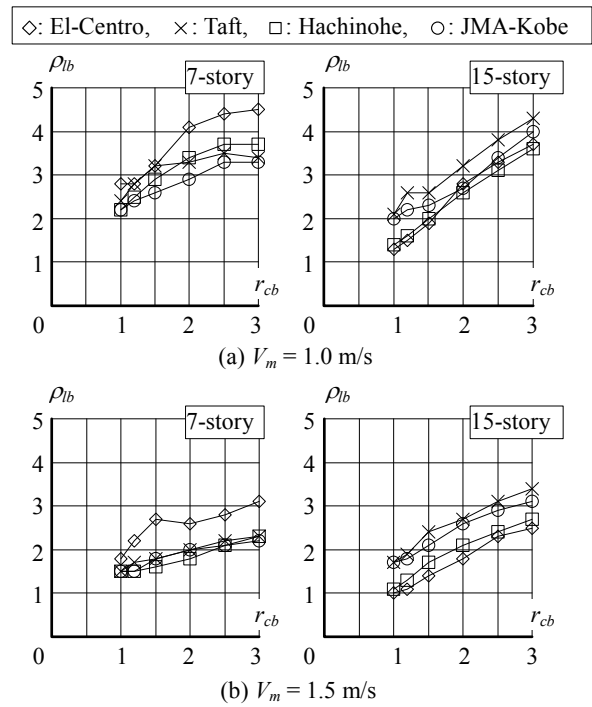


Figure 7.1 Lower bound of the strength ratio in case the local buckling of CFT column occurs

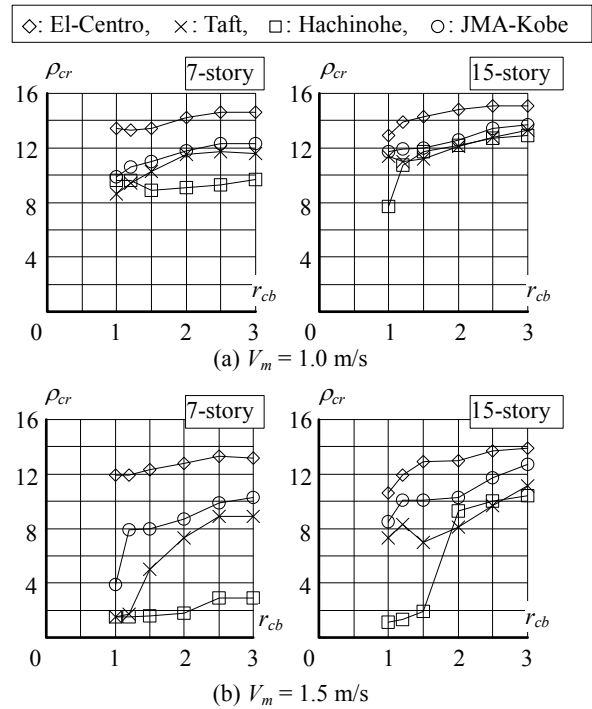


Figure 7.2 Lower bound of the strength in case the steel tube cracking of CFT column occurs

7. NO DAMAGE LIMIT OF STRENGTH RATIO OF CFT COLUMN

To avoid the local buckling and steel tube cracking of CFT column subjected to strong seismic load, the design limits of the strength ratio of filled concrete to steel tube (ρ_{lb} , ρ_{cr}) are investigated. Fig.7.1 shows the lower bound values of strength ratio of filled concrete to steel tube in case the local buckling of CFT column occurs (ρ_{lb}). The input ground motions are amplified the maximum velocity (V_m) to $V_m = 1.0$ or 1.5 m/s. According to Fig. 7.1, ρ_{lb} increases with the column-over-design factor (r_{cb}) monotonically in each ground motion.

Fig. 7.2 shows the lower bounds of the strength ratio of filled concrete to steel tube in case the steel tube cracking of CFT column occurs (ρ_{cr}). According to Fig. 7.2, ρ_{cr} also tends to increase with r_{cb} . However, ρ_{cr} are affected by the ground motion because of the duration of ground motion and the number of cyclic load (Hachinohe wave has long duration and many load cycles).

8. CONCLUSIONS

Seismic responses and damages of many CFT frames under strong ground motions have been analyzed and it is pointed out that not only the ultimate story shear strength and the shear strength distribution but also the column-over-design factor (r_{cb}) and the strength ratio of filled concrete to steel tube (ρ) affect both damage ratios of the local buckling and the steel tube cracking strongly. The distribution of r_{cb} also affects the damage of CFT frame strongly. Especially, the sudden r_{cb} change and the distribution that r_{cb} increase from the first story linearly provide not safe design condition. On the other hand, the distribution that r_{cb} decrease from the first story linearly provide safe design condition. However, these design condition related to the r_{cb} distribution are supposed to be changed by the number of story and the input ground motion. These points become next future subjects.

To prevent the local buckling and the steel tube cracking of CFT column, the lower bounds of the strength ratio of filled concrete to steel tube in case these damages occur (ρ_{lb} , ρ_{cr}) are investigated quantitatively. From these results, although both ρ_{lb} and ρ_{cr} vary according to r_{cb} and the maximum velocity of input ground motion (V_m), the strength ratio of filled concrete to steel tube should be less than 1.0 to prevent the local buckling and steel tube cracking of CFT frame under strong ground motion.

REFERENCES

- Clough, R.W. & Johnston, S.B. (1966), Effect of stiffness degradation on earthquake ductility requirements, *Proceedings of Japan Earthquake Engineering Symposium*, 227-232.
- Dowling, N.E. (2007), *Mechanical Behavior of Materials*, Person Prentice Hall.
- Goto, K. (2010), Crack fracture type of H-section cantilever beam under strong cyclic load, *Proceedings of 9th Pacific Structural Steel Conference*, 1017-1023.
- Goto, K. & Saisho, M. (2010), Crack damage of multi-story CFT frame under strong motion, *Proceedings of the 13th International Symposium on Tubular Structures*, 149-157
- Saisho, M. & Goto, K. (2001), Restoring force model of concrete filled steel tube column under seismic load, *Proceedings of the 9th Pacific Structural Steel Conference*, 453-458.
- Saisho, M. & Goto, K. (2004), Ultimate earthquake resistant capacity of CFT-frame, *Proceedings of the 13th World Conference on Earthquake Engineering*, Paper No.2613.
- Saisho, M., Kato, M. & Gao, S. (2004) Local buckling of CFT-column under seismic load, *Proceedings of the 13th World Conference on Earthquake Engineering*, Paper No.2614.